J|A|C|S
ARTICLES
Published on Web 01/10/2007

The Carboxylate Shift in Zinc Enzymes: A Computational Study

Sérgio F. Sousa, Pedro A. Fernandes, and Maria João Ramos*

Contribution from REQUIMTE, Departamento de Química, Faculdade de Ciências, Universidade do Porto, Rua do Campo Alegre, 687, 4169-007 Porto, Portugal

Received October 4, 2006; E-mail: mjramos@fc.up.pt

Abstract: Zinc is the second most abundant transition element in biology and the only metal known to be represented in enzymes from each one of the six classes established by the International Union of Biochemistry. The flexible coordination geometry, the fast ligand exchange, the lack of redox activity, and its role as Lewis acid are just some of the features that make zinc an invaluable element in biological catalysis. In this study, we have analyzed the importance in mononuclear Zn enzymes of an interesting mechanistic phenomenon known as carboxylate shift, which is characterized by a change in the coordination mode of a carboxylate group (mono to bidentate or vice versa) with both ligand entrance or exit from the metal coordination sphere. Using B3LYP calculations, we were able to unveil in detail patterns relating the intrinsic characteristics of a given Zn coordination sphere with the existence or not of a carboxylate-shift mechanism and the additional energy stabilization arising from it. In particular, a specific Zn coordination sphere containing a carboxylate ligand (Asp or Glu), a cysteine, and a histidine has been shown to have the most favorable combination of amino acid residues that ensures a fast ligand exchange.

Introduction

Zinc, the second most abundant transition element in biology (after iron), is an integral component of more than 400 enzymes involved in virtually all aspects of metabolism and present in a broad array of species of all phyla.[1−3] The RNA polymerase II,[4−8] the matrix metalloproteinases,[9−11] and the metallo-β-lactamases[12,13] are among the most discussed examples in recent years, but the list of zinc metalloenzymes and metalloproteins comprises an extremely diversified plethora of interesting cases, such as the carboxypeptidases, the aminopeptidases, the thermolysins, the carbonic anhydrases, the alcohol dehydrogenases,[3,14] some classical intriguing systems, such as the signaling protein Sonic hedgehog,[15,16] and the puzzling enzyme farnesiltransferase.[17−22] In fact, zinc is the only metal known to be represented in enzymes from each one of the six classes established by the International Union of Biochemistry,[2] and a recent bioinformatics survey on the Zn proteins encoded in the human genome has proposed that ca. 2800 human proteins are potentially zinc binding in vivo, a number that represents approximately 10% of the total human proteome.[23]

Typically, the metal coordination environment in mononuclear Zn enzymes where the metal atom is involved in catalysis is a distorted tetrahedron containing three amino acid side chain ligands and a small molecule.[3] Histidine is the most common ligand, followed by glutamate, aspartate, and cysteine.[1,24] To understand the almost ubiquitous presence of zinc in organisms and the structure, function, and mechanism of zinc enzymes, the very special nature of this metal has to be taken into account. In reality, zinc has very particular characteristics that detach it from the other first-row transition metals and that make zinc very attractive for biological systems. The flexible coordination geometry, the fast ligand exchange, the lack of redox activity, and its role as Lewis acid are just a few examples that add to a high bioavailability.[3,25] However, despite the very important functions that several zinc enzymes perform, several significant questions remain unanswered.

In this study, we analyze an interesting mechanistic phenomenon known as carboxylate shift, which is characterized by a

(1) Vallee, B. L.; Auld, D. S. *Biochemistry* **1990**, *29*, 5647.
(2) Vallee, B. L.; Auld, D. S. *Proc. Natl. Acad. Sci. U.S.A.* **1990**, *87*, 220.
(3) Lipscomb, W. N.; Strater, N. *Chem. Rev.* **1996**, *96*, 2375.
(4) Hahn, S. *Nat. Struct. Mol. Biol.* **2004**, *11*, 394.
(5) Bushnell, D. A.; Westover, K. D.; Davis, R.; Kornberg, R. D. *Science* **2004**, *303*, 983.
(6) Donaldson, I. M.; Friesen, J. D. *J. Biol. Chem.* **2000**, *275*, 13780.
(7) Gnatt, A. L.; Fu, J.; Bushnell, D. A.; Kornberg, R. D. *Science* **2001**, *292*, 1876.
(8) Cramer, P.; Bushnell, D. A.; Kornberg, R. D. *Science* **2001**, *292*, 1863.
(9) Brinckerhoff, C. E.; Matrisian, L. M. *Nat. Rev. Mol. Cell Biol.* **2002**, *3*, 207.
(10) Egeblad, M.; Werb, Z. *Nat. Rev. Cancer* **2002**, *2*, 161.
(11) Coussens, L. M.; Fingleton, B.; Matrisian, L. M. *Science* **2002**, *295*, 2387.
(12) Cricco, J. A.; Vila, A. J. *Curr. Pharm. Des.* **1999**, *5*, 915.
(13) Heinz, U.; Adolph, H. W. *Cell. Mol. Life Sci.* **2004**, *61*, 2827.
(14) Coleman, J. E. *Curr. Opin. Chem. Biol.* **1998**, *2*, 222.
(15) Day, E. S.; et al. *Biochemistry* **1999**, *38*, 14868.
(16) Hall, T. M.; Porter, J. A.; Beachy, P. A.; Leahy, D. J. *Nature* **1995**, *378*, 212.
(17) Long, S. B.; Casey, P. J.; Beese, L. S. *Nature* **2002**, *419*, 645.
(18) Park, H. W.; Boduluri, S. R.; Moomaw, J. F.; Casey, P. J.; Beese, L. S. *Science* **1997**, *275*, 1800.
(19) Sousa, S. F.; Fernandes, P. A.; Ramos, M. J. *J. Mol. Struct.: THEOCHEM* **2005**, *729*, 125.
(20) Sousa, S. F.; Fernandes, P. A.; Ramos, M. J. *J. Biol. Inorg. Chem.* **2005**, *10*, 3.
(21) Sousa, S. F.; Fernandes, P. A.; Ramos, M. J. *Biophys. J.* **2005**, *88*, 483.
(22) Tobin, D. A.; Pickett, J. S.; Hartman, H. L.; Fierke, C. A.; Penner-Hahn, J. E. *J. Am. Chem. Soc.* **2003**, *125*, 9962.
(23) Andreini, C.; Banci, L.; Bertini, I.; Rosato, A. *J. Proteome Res.* **2006**, *5*, 196.
(24) Alberts, I. L.; Nadassy, K.; Wodak, S. J. *Protein Sci.* **1998**, *7*, 1700.
(25) McCall, K. A.; Huang, C. C.; Fierke, C. A. *J. Nutr.* **2000**, *130*, 1437.

10.1021/ja067103n CCC: $37.00

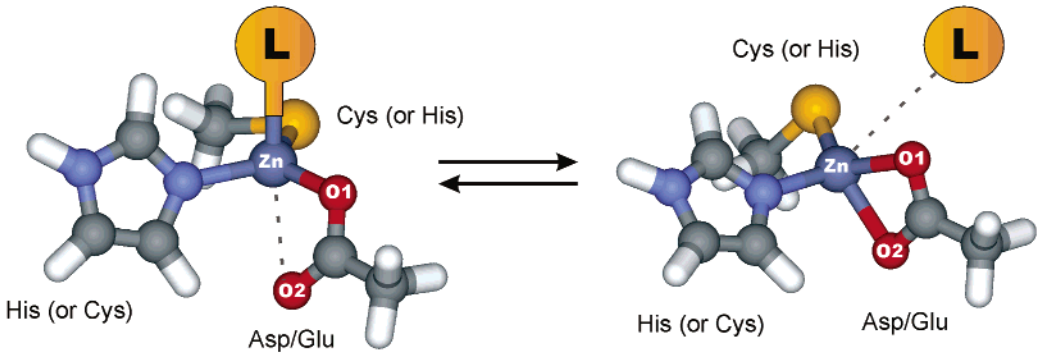

Figure 1. Schematic representation of the carboxylate-shift mechanism in typical mononuclear Zn enzymes, illustrating the combinations of amino acid residues tested and the type of models considered. The ligands L tested were H_2O, CH_3OH, CH_3OCH_3, CH_3SH, and CH_3SCH_3.

change in the coordination form of a carboxylate group. In mononuclear systems, this change takes typically the form of a monodentate to bidentate change with ligand exit, or vice versa with ligand entrance (Figure 1). The ability of the carboxylate group to rearrange in such a manner allows a constant or nearly constant coordination number to be maintained throughout an entire catalytic pathway of a given enzyme, providing an efficient mechanism to lower the activation barriers for ligand exit or entrance processes. In polynuclear systems, such changes can take more complex forms, cycling between monodentate terminal, bidentate chelating, monodentate bridging (μ-1,1), and bidentate bridging (μ-1,2) coordination modes,[26] but the outcome is basically the same: easy interchange of ligands and extremely high flexibility of the Zn coordination sphere. Farnesyltransferase (FTase) is probably the most representative example of a mononuclear enzyme where a carboxylate-shift mechanism has been suggested.[19−21,27] Notable examples of polynuclear biological systems where this type of phenomena has been reported include the R2 subunit of ribonucleotide reductase[28−31] and the methane monooxygenase enzyme,[31,32] two extremely well-studied diiron enzymes. This type of phenomena has also been observed in a number of model compounds containing Fe,[33−35] Mn,[35−37] Cd,[38] and Zn.[26]

In this particular study, we have analyzed the influence of the carboxylate-shift mechanism in Zn enzymes, more specifically in the process of exit from the metal coordination sphere of five different molecules representing five different classes of compounds. These were H_2O, an alcohol (CH_3OH), an ether (CH_3OCH_3), a thiol (CH_3SH), and a thioether (CH_3SCH_3). Water is an almost universally present and critical component in catalytically active Zn sites and by far the most common element in this type of metal sphere.[2] In fact, 92% of the catalytic Zn sites available in the PDB are thought to contain a Zn-bound water or a Zn-bound inhibitor replacing water in the primary coordination sphere.[24] Zn-bound alcohols, ethers, thiols, and thioethers are also typically formed in the intermediate steps of several reactions catalyzed by Zn enzymes.[3] All the possible combinations of a tetracoordinated Zn center containing one of these five small molecules together with a single carboxylate ligand (Asp or Glu) were analyzed in this study (His−His−ligand−carboxylate, His−Cys−ligand−carboxylate, Cys−Cys−ligand−carboxylate). Features such as the nature and identity of the ligands in the Zn coordination sphere, their relationship with the existence of a carboxylate-shift mechanism, and the Gibbs activation and reaction energies for ligand exit were the subject of particular attention. Basically, we aimed to unravel trends and patterns relating these features to the intrinsic characteristics of a given Zn coordination sphere using high-level theoretical methods at the density functional theory (DFT) level of theory; in real biological systems, these aspects will be further influenced by the specific enzymatic environment surrounding each metal center.

Methodology

As pointed out in the Introduction, the metal coordination environment in mononuclear Zn enzymes involved in catalysis typically contains three amino acid side chains ligands (His, Glu, Asp, and Cys) plus a small molecule, defining a distorted tetrahedron[3] (Figure 1). To study in detail the importance of the carboxylate-shift effect in mononuclear Zn systems, we decided to focus our attention on Zn coordination spheres that contain solely one carboxylate ligand (Asp, Glu), which according to the characteristics described above yields three possible combinations of ligands at the Zn coordination sphere, if both Asp and Glu residues are described by generic carboxylate ligand. These combinations are His−His−ligand−carboxylate, His−Cys−ligand−carboxylate, and Cys−Cys−ligand−carboxylate. These different coordination spheres were labeled, respectively, case 1, case 2, and case 3 spheres. For each of these three distinct Zn environments, the displacement processes of five different neutral molecules representing five different classes of compounds were analyzed. These were H_2O, an alcohol (CH_3OH), an ether (CH_3OCH_3), a thiol (CH_3SH), and a thioether (CH_3SCH_3).

Starting from the crystallographic structure of the FTase resting state (1FT1)[18] (His−Cys−H_2O−carboxylate), each one of the initial structures for the 15 case studies described above (three combinations of ligands with five different initial molecules each) were prepared and

(26) Demsar, A.; Kosmrlj, J.; Petricek, S. *J. Am. Chem. Soc.* **2002**, *124*, 3951.
(27) Sousa, S. F.; Fernandes, P. A.; Ramos, M. J. *Theor. Chem. Acc.*, published online Oct 6, 2006, http://dx.doi.org/10.1007/s00214-006-0170-9.
(28) Assarsson, M.; Andersson, M. E.; Hogbom, M.; Persson, B. O.; Sahlin, M.; Barra, A. L.; Sjoberg, B. M.; Nordlund, P.; Graslund, A. *J. Biol. Chem.* **2001**, *276*, 26852.
(29) Hogbom, M.; Andersson, M. E.; Nordlund, P. *J. Biol. Inorg. Chem.* **2001**, *6*, 315.
(30) Andersson, M. E.; Hogbom, M.; Rinaldo-Mathis, A.; Andersson, K. K.; Sjoberg, B. M.; Nordlund, P. *J. Am. Chem. Soc.* **1999**, *121*, 2346.
(31) Torrent, M.; Musaev, D. G.; Morokuma, K. *J. Phys. Chem. B* **2001**, *105*, 322.
(32) Gherman, B. F.; Baik, M. H.; Lippard, S. J.; Friesner, R. A. *J. Am. Chem. Soc.* **2004**, *126*, 2978.
(33) Lemercier, G.; Mulliez, E.; Brouca-Cabarrecq, C.; Dahan, F.; Tuchagues, J. P. *Inorg. Chem.* **2004**, *43*, 2105.
(34) Kuzelka, J.; Spingler, B.; Lippard, S. J. *Inorg. Chim. Acta* **2002**, *337*, 212.
(35) Rardin, R. L.; Bino, A.; Poganiuch, P.; Tolman, W. B.; Liu, S.; Lippard, S. J. *Angew. Chem., Int. Ed.* **1990**, *102*, 812.
(36) Baffert, C.; Collomb, M. N.; Deronzier, A.; Kjaergaard-Knudsen, S.; Latour, J. M.; Lund, K. H.; McKenzie, C. J.; Mortensen, M.; Nielsen, L.; Thorup, N. *J. Chem. Soc., Dalton Trans.* **2003**, *9*, 1765.
(37) Pursche, D.; Triller, M. U.; Reddig, N.; Rompel, A.; Krebs, B. *Z. Anorg. Allg. Chem.* **2003**, *629*, 24.
(38) Zheng, S. L.; Li, W.; Yang, G.; Zhu, H. G.; Ye, B. H.; Chen, X. M. *Aust. J. Chem.* **2002**, 611.

optimized. Conventional modeling of the amino acid side chains was used, that is, the zinc ligands aspartate (or glutamate), cysteinate, and histidine were modeled by acetate, methylthiolate, and imidazole, respectively. The validity of this type of approach has been demonstrated before in the mechanistic study of FTase[19,21,39] and of several different enzymes.[40−45] The geometry of each model was first freely optimized. Several starting structures were tested to avoid the risk of being trapped in local minima. These starting structures were prepared by changing the orientation of the several ligands in relation to the zinc atom while keeping acceptable Zn−ligand initial distances. No geometric constraints were imposed on any of the calculations. The obtained minima were then characterized from the structural point of view (Figure 2). Subsequently, a scan along the Zn−L distance for each one of the models was performed by successively increasing this distance at 0.05 Å intervals and reoptimizing the model. A total of 100 geometries were considered in each scan. From the resulting potential energy surfaces, two or three minima connected by one or two transition states were identifiable for each scan. The maxima obtained were used as starting guesses to find the corresponding transition states. The transition state structures were later freely optimized. An identical procedure was followed for the several energy minima. Frequency analyses were performed at each stationary point on the potential energy surface. Therefore, all the minima and transition states were verified, taking into account the number of imaginary frequencies. To fully evaluate the role played by the carboxylate shift in ligand exit, the entire procedure described above was repeated while freezing in each scan the longer Zn−carboxylate distance (Zn−O2), thereby preventing the occurrence of energy stabilization in ligand exit through a carboxylate-shift mechanism. Even though it is well-known that performing frequency calculations on constrained systems is inaccurate from the mathematical point of view, for the particular problem at hand, where the same Zn−O2 bond is kept frozen in all stationary points, this procedure provides a very reasonable approximation to target the importance of the carboxylate-shift effect, by comparison with the free system. Altogether, a total of 13 free and 13 frozen scans were performed, comprising 56 energy minima, 29 transition states, and around 1300 intermediate geometries.

In all the calculations described above, DFT with the B3LYP functional[46,47] was used. DFT calculations have been shown to give very accurate results for systems involving transition metals,[48] particularly when using the B3LYP functional.[49−51] For zinc complexes, the superior accuracy of the B3LYP functional in comparison with Hartree−Fock and second-order Moller−Plesset perturbation theory has also been previously demonstrated.[42] For this study, the accuracy of the B3LYP functional in the treatment of this type of Zn complex was tested for both geometry optimizations and energy calculations against the B1B95, B97-2, BP86, and BPW91 functionals. In the set of geometry optimizations performed, B3LYP gave the most accurate results. Furthermore, from the energy calculations no significant differences between the faster B3LYP and the other functionals tested were observed. These results validate the use of B3LYP for the present work. Details are presented in the Supporting Information.

Optimizations were carried out using the SDD basis set, as implemented in Gaussian 03.[52] This basis set uses the small core *quasi*-relativistic Stuttgart/Dresden electron core potentials (also known as Stoll-Preuss, or simply SP)[53,54] for transition elements. For zinc, the outer electrons are described by a (311111/22111/411) valence basis specifically optimized for this metal and for the use with the SP pseudopotentials. C, N, and O atoms are accounted by a (6111/41) quality basis set, whereas S and H atoms are treated, respectively, by a (531111/4211) and a (31) quality basis sets. The high performance of SP pseudopotentials in calculations involving transition metal compounds, particularly within closed-shell systems, has been previously demonstrated.[55] This basis set has also been used before with B3LYP in the study of FTase.[19,21,39]

A polarized continuum model (the IEF-PCM, as implemented in Gaussian 03[56−59]) was subsequently used to calculate the energy values, simulating a generic enzymatic environment and allowing the long-range, nonspecific, isotropic effects to be accounted for. This model has been shown to give better results for low dielectric constants than the alternative model C-PCM,[60] a feature that is of particular importance to the study of enzymatic catalysis, since the use of a *continuum* model is normally taken as an approximation of the effect of the global enzyme environment in a reaction, having been shown, in previous studies on active sites in proteins[40,61−63] that an empirical dielectric constant (ϵ) of 4 gives generally good agreement with experimental results and accounts for the average effect of both the protein and buried water molecules. Previous studies have demonstrated that the effect of the *continuum* in geometries is, in general, rather small, even in charged systems.[64,65] Therefore, in all PCM calculations, it was assumed that gas-phase geometries could be transferred without the introduction of significant errors. IEF-PCM energy calculations with B3LYP/6-311++G(3df,3pd) were performed for all minima, as well as for the transition states. Zero-point corrections, thermal, and entropic effects ($T = 310.15$ K, $P = 1$ bar) calculated in vacuum at the B3LYP/SDD level were added to all calculated energies. All calculations were performed using the Gaussian 03 software package.[52]

Results and Discussion

1. Initial Minima. All the initial minima obtained for each of the combinations of a Zn coordination sphere with a small molecule L, as described in the previous section, are presented in Figure 2. We would like to stress, once again, that for each minimum several starting structures were tested by varying the orientation of the several ligands in relation to the Zn atom while keeping acceptable Zn−ligand initial distances, as to reduce the risk of being trapped in local minima. For 13 of the 15 combinations, a monodentate minima with a Zn-bound (or at least directly interacting) ligand L was obtained. The only two

(39) Sousa, S. F.; Fernandes, P. A.; Ramos, M. J. *Proteins: Struct., Funct., Bioinf.* **2007**, *66*, 205.
(40) Siegbahn, P. E. M. *J. Am. Chem. Soc.* **1998**, *120*, 8417.
(41) Melo, A.; Ramos, M. J.; Floriano, W. B.; Gomes, J. A. N. F.; Leão, J. F. R.; Magalhães, A. L.; Maigret, B.; Nascimento, M. C.; Reuter, N. *J. Mol. Struct.: THEOCHEM* **1999**, *463*, 81.
(42) Ryde, U. *Biophys. J.* **1999**, *77*, 2777.
(43) Fernandes, P. A.; Ramos, M. J. *J. Am. Chem. Soc.* **2003**, *125*, 6311.
(44) Fernandes, P. A.; Ramos, M. J. *Chem.−Eur. J.* **2003**, *9*, 5916.
(45) Pereira, S.; Fernandes, P. A.; Ramos, M. J. *J. Comput. Chem.* **2004**, *25*, 227.
(46) Lee, C.; Yang, W. T.; Parr, R. G. *Phys. Rev. B* **1988**, *37*, 785.
(47) Becke, A. D. *J. Chem. Phys.* **1993**, *98*, 5648.
(48) Ziegler, T. *Chem. Rev.* **1991**, *91*, 651.
(49) Bauschlicher, C. W. *Chem. Phys. Lett.* **1995**, *246*, 40.
(50) Holthausen, M. C.; Mohr, M.; Koch, W. *Chem. Phys. Lett.* **1995**, *240*, 245.
(51) Ricca, A.; Bauschlicher, C. W. *Theor. Chim. Acta* **1995**, *92*, 123.
(52) Frisch, M. J.; et al. *Gaussian 03*, revision C.02; Gaussian, Inc.: Wallingford, CT, 2004.
(53) Dolg, M.; Wedig, U.; Stoll, H.; Preuss, H. *J. Chem. Phys.* **1987**, *86*, 866.
(54) Andrae, D.; Haussermann, U.; Dolg, M.; Stoll, H.; Preuss, H. *Theor. Chim. Acta* **1990**, *77*, 123.
(55) Frenking, G.; Antes, I.; Bohme, M.; Dapprich, S.; Ehlers, A. W.; Jonas, V.; Neubaus, A.; Otto, M.; Stegmann, R.; Veldkamp, A.; Vyboishchikov, S. F. *Rev. Comput. Chem.* **1996**, *8*, 63.
(56) Cances, E.; Mennucci, B.; Tomasi, J. *J. Chem. Phys.* **1997**, *107*, 3032.
(57) Mennucci, B.; Tomasi, J. *J. Chem. Phys.* **1997**, *106*, 5151.
(58) Cossi, M.; Barone, V.; Mennucci, B.; Tomasi, J. *Chem. Phys. Lett.* **1998**, *286*, 253.
(59) Cossi, M.; Scalmani, G.; Rega, N.; Barone, V. *J. Chem. Phys.* **2002**, *117*, 43.
(60) Cossi, M.; Rega, N.; Scalmani, G.; Barone, V. *J. Comput. Chem.* **2003**, *24*, 669.
(61) Blomberg, M. R. A.; Siegbahn, P. E. M.; Babcock, G. T. *J. Am. Chem. Soc.* **1998**, *120*, 8812.
(62) Siegbahn, P. E. M.; Eriksson, L. A.; Himo, F.; Pavlov, M. *J. Phys. Chem. B* **1998**, *102*, 10622.
(63) Cerqueira, N. M. F. S. A.; Fernandes, P. A.; Eriksson, L. A.; Ramos, M. J. *Biophys. J.* **2006**, *90*, 2109.
(64) Fernandes, P. A.; Eriksson, L. A.; Ramos, M. J. *Theor. Chem. Acc.* **2002**, *108*, 352.
(65) Fernandes, P. A.; Ramos, M. J. *Chem.−Eur. J.* **2004**, *10*, 257.

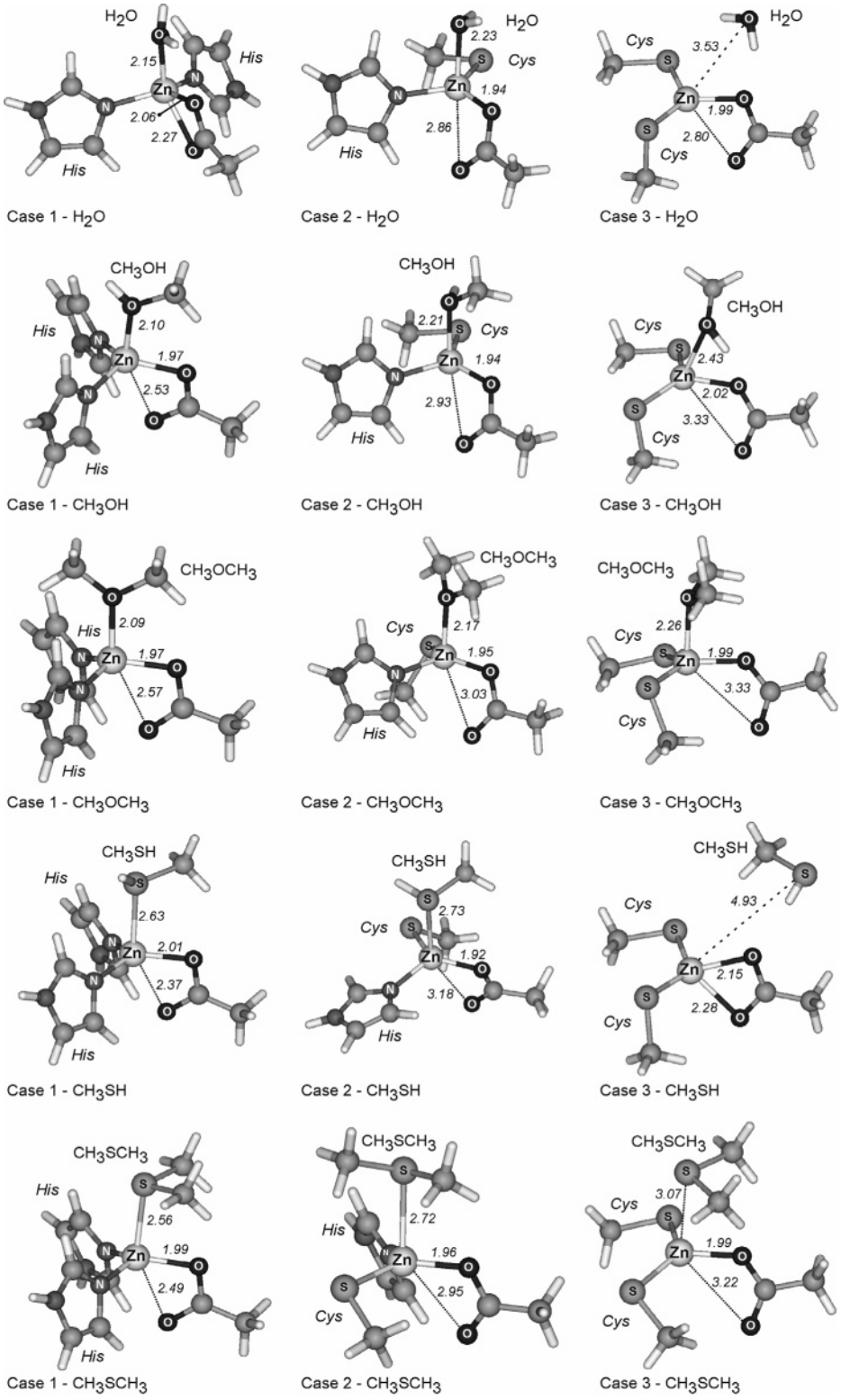

Figure 2. Initial minima obtained for each combination of one of the five ligands L with the three different Zn coordination environments studied: case 1, case 2, and case 3 coordination spheres. Critical bond lengths are reported in angstroms.

exceptions were for the case 3 sphere, with the ligands H_2O and CH_3SH, where despite all attempts no such minima were obtained. In these two cases, the geometry optimizations of all the starting structures tried resulted in the unbound minima represented in Figure 2.

Figure 3 presents a relation of the two critical bond lengths in the 13 initial Zn-bound minima described in Figure 2. These bond lengths are the Zn−L and the Zn−O2 distances, where L and O2 refer, respectively, to the small molecule considered and to the oxygen atom from the carboxylate group that is located further away from the Zn center. We aimed to see how these two lengths varied with the nature of the Zn coordination sphere, taking into consideration that for cases 1, 2, and 3 the overall charges are +1, 0, and −1, respectively. As expected,

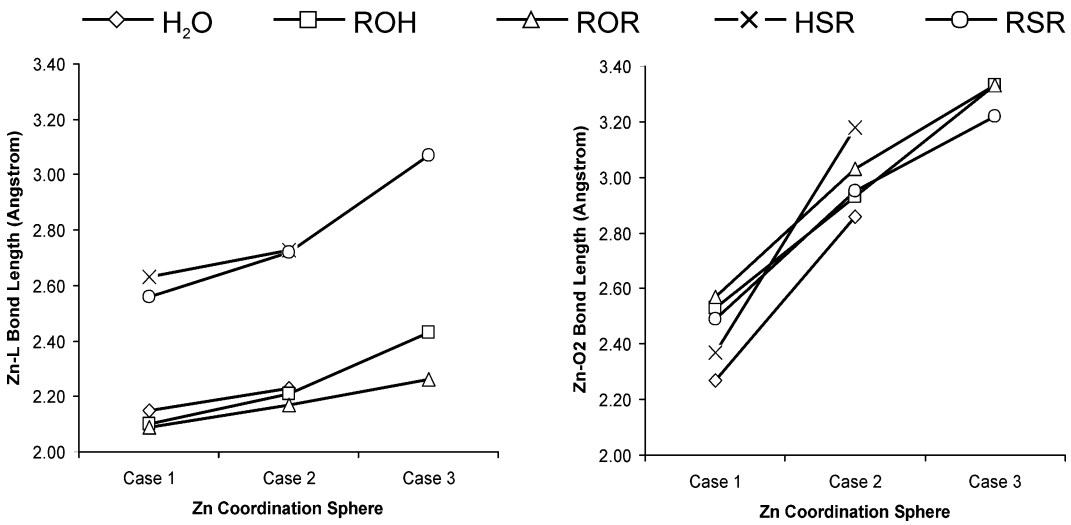

Figure 3. Relation of the most relevant Zn−ligand bond lengths with the nature of the Zn coordination sphere for the 13 Zn-bound minima described in Figure 2. R corresponds to a CH_3 group.

there is a natural increase in these two distances as the overall charge of the complex decreases and the central Zn cation becomes less positive. The length of the only other Zn bond that is present in all the structures (the Zn−O1 bond) does not follow the same pattern, as can be seen from the analysis of Figure 2. An interesting pattern also visible in the initial minima represented in Figure 2 is that for the case 1 sphere: the Zn−O1 and Zn−O2 distances have much closer lengths than those in case 2 and this difference is typically larger in case 3. Hence, the Zn-bound minima in the case 1 sphere all have a much smaller monodentate character and can even be considered in some of the cases to be, at least to some extent, bidentate.

2. Structural Alterations with Ligand Exit. An important structural feature in terms of the carboxylate-shift mechanism that is particularly visible in Figure 3 is the relation of the Zn−O2 bond length with the nature of the coordination sphere. For the case 1 sphere, the Zn−O2 distances for the five ligands all fall within a 2.20−2.60 Å interval, whereas for the case 2 sphere these values are in a 2.80−3.20 Å interval. For the case 3 sphere, the three Zn-bound minima have Zn−O2 values all higher than 3.20 Å.

Figure 4 further relates the module of the difference between the Zn−O1 and Zn−O2 bond lengths (the two carboxylate oxygens) with the ligand (L) exit. In most systems studied, it is obvious that, as the ligand L is displaced from the Zn coordination sphere, there is a decrease in the Zn−O2 distance and the carboxylate group changes from mono to bidentate (carboxylate shift), as illustrated in Figure 1. Exceptions to this behavior comprise the cases where the initial difference between the Zn−O1 and Zn−O2 distances exceeds 1.20 Å (Figure 4), which implies initial Zn−O2 distances in the order of 3.20 Å or higher (as indicated in Figure 3). The systems that do not suffer a mono to bidentate carboxylate-shift mechanism include the case 2 sphere with the CH_3SH molecule and the case 3 sphere with the CH_3OCH_3 and CH_3SCH_3 molecules, where the initial Zn−O2 values are very high. For the CH_3OH molecule in the case 3 sphere, there is also not a mono to bidentate change, but rather a change in the carboxylate oxygen atom that is Zn-coordinated, taking place without the existence of an intermediate bidentate minimum. This type of change is also partially observable in the case of the H_2O molecule for both cases 1 and 2 coordination spheres, due to formation of a strong hydrogen bond of the leaving group (L) to the carboxylate oxygen atom initially closer to Zn. However, in these two situations the change takes place through the existence of one or more bidentate minima and hence is formally preceded by a mono to bidentate carboxylate shift.

The variation of all the individual Zn distances with ligand exit for the several coordination spheres (cases 1, 2, and 3) and ligands L is presented in the Supporting Information.

3. Gibbs Activation Barriers. The Gibbs activation barriers for ligand exit in each one of these 13 systems are presented in Figure 5 (free carboxylate). This figure also presents the values calculated for the processes of ligand exit where the carboxylate-shift mechanism was prevented by freezing the initial Zn−O2 distance (frozen carboxylate). As already discussed, for the case 3 sphere with the ligands H_2O and CH_3SH, only the unbound minima were obtained. For the free processes, the case 1 sphere tends to have much higher barriers for ligand exit than cases 2 and 3, which is in agreement with the existence of stronger and shorter Zn−L bonds for case 1 as a result of a larger positive charge at the Zn cation, as indicated in Figure 3 and previously discussed.

Figure 6 shows the difference in the Gibbs activation barriers for ligand exit with a free and a frozen carboxylate group for the several coordination spheres and ligands studied. From the analysis of Figures 5 and 6, it is possible to evaluate the importance of the carboxylate-shift mechanism in the systems considered. For the case 3 sphere, having a free or a frozen carboxylate has almost no effect on the activation barrier, which agrees with the fact that no mono to bidentate carboxylate shift was observed (Figure 4). Case 1 exhibits the largest differences in the calculated activation barriers with a free and a frozen carboxylate group for almost all the molecules studied, with differences typically around 5−7 kcal/mol, whereas for case 2 these differences fall within a 3−5 kcal/mol. The only significant exception encountered was the water molecule, for which the obtained frozen−free difference in the case 2 sphere was more than two times higher than that in case 1 (1.37 and 3.78 kcal/mol, respectively, in cases 1 and 2). In terms of the relative values, the opposite trend is observed, as case 2 exhibits the lowest free Gibbs activation barriers. In fact, in the case of H_2O

and CH_3OH exit for the case 2 sphere, blocking this mechanism induces an almost 7-fold increase in the Gibbs activation barriers (from 0.57 and 0.63 kcal/mol to 4.38 and 4.82 kcal/mol, respectively), whereas for CH_3OCH_3 and CH_3SCH_3 this increase is 1- to 2-fold. For the case 1 sphere, the maximum destabilization was 2-fold.

4. Relative Stability of the Zn-Bound and Zn-Unbound Minima. Figure 7 presents the Gibbs reaction energies for ligand exit for all the combinations of ligands studied. From an analysis of this figure, some clear tendencies are easily observed. For the case 1 sphere, the bound minima are clearly favored over the unbound alternative. For the case 2 sphere, the outcome depends on the identity of the ligand L, whereas in case 3 the unbound minima are normally more stable. This last conclusion can be further reinforced by the fact that for both the H_2O and CH_3SH molecules in the case 3 sphere only the unbound minima were obtained (Figure 2). Altogether, the difference between a Zn-bound and a Zn-unbound minimum for a given ligand L tends to be smaller for the case 2 coordination sphere, whereas in case 3 these differences are the highest. In most cases, the differences between the Zn-bound and Zn-unbound minima are very small, especially when there is a carboxylate shift involved, and therefore, the two states will tend to exist in equilibrium at room temperature.

The relative Gibbs energies calculated for all the 85 stationary states determined from both free and frozen scans for all five ligands and three coordination environments are presented in the Supporting Information.

5. The Carboxylate-Shift: Trends and Implications. From the set of results described above, several interesting conclusions arise concerning both the nature and structure of the Zn coordination sphere and the outcome of the ligand displacement processes.

The case 1 Zn coordination sphere, which comprises a carboxylate amino acid ligand and two His residues (charge +1), has some very specific characteristics that detach it from the other two Zn environments. For this type of sphere, the coordination of small molecules tends to be stronger than in the other Zn spheres, with shorter bond lengths and higher barriers for ligand exchange (at least twice as high as for case 2). The carboxylate shift has an energetic impact typically around 2.8−7.0 kcal/mol, lowering the Gibbs activation barriers to values between 3.9 and 7.0 kcal/mol. The exit process in the absence of specific interactions by the enzyme is endothermic for all ligands. These features make this sphere less prone to ligand exchange than the case 2 combination. The case 1 sphere is the most typical Zn coordination environment in Zn catalytic sites, present in a wide range of biological systems. Examples include carboxypeptidase A, thermolysin, pseudolysin, bacillolysin, β-lactamase, and the Sonic hedgehog.[3,14,24]

The Zn coordination sphere defined in case 2, which comprises a carboxylate ligand plus a single histidine and a single cysteine (overall charge 0), has both the lowest Gibbs activation barriers for ligand exchange and the smallest energy difference between the Zn-bound and unbound minima, therefore acting as the best combination of amino acid ligands to ensure a fast ligand exchange. In fact, in general, in no other combination of residues were such favorable features encountered. Particularly interesting is also the fact that these trends were observed for the entire set of five ligands studied,

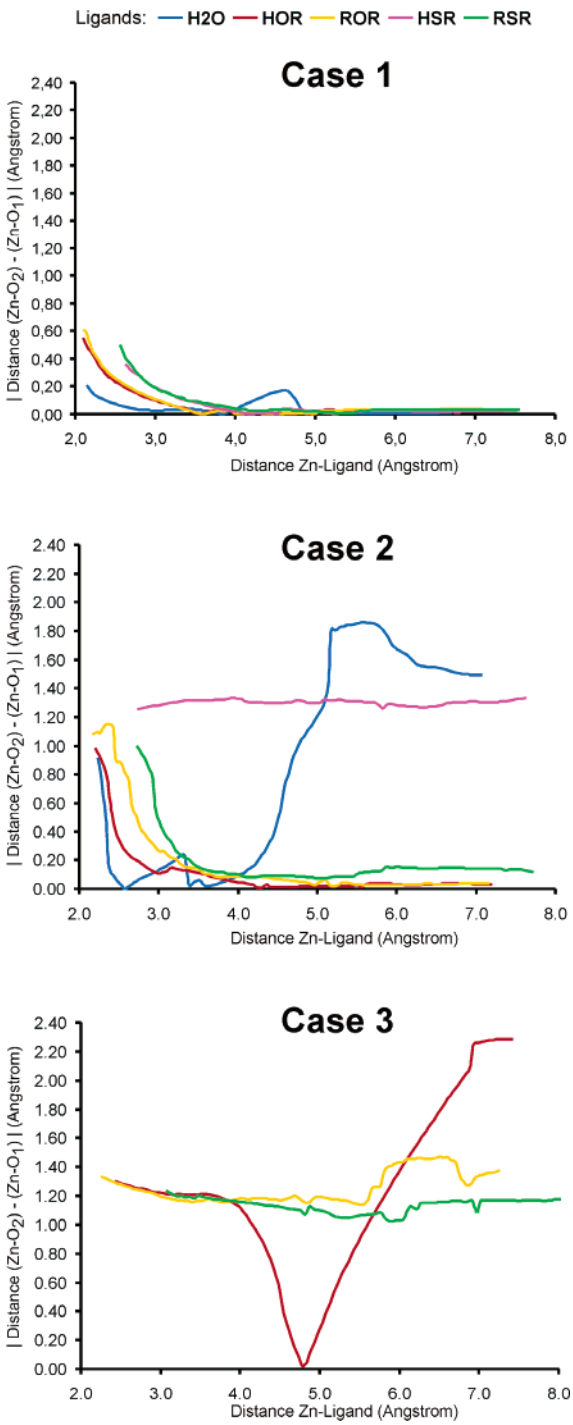

Figure 4. Module of the difference in the bond lengths between Zn and the two oxygen atoms from the carboxylate group for the several coordination spheres and ligands studied. R corresponds to a CH_3 group.

comprising water, alcohol, ether, thiol, and thioether molecules. In fact, for this coordination sphere the carboxylate shift enables a stabilization of the Gibbs activation barriers for ligand exit of 2.9 to 4.8 kcal/mol, resulting in free activation barriers of 0.6 to 2.6 kcal/mol. These characteristics make it the coordination sphere of excellence for enzymes that require an easy exchange of ligands or that coordinate to substrates with different functional groups during their catalytic pathway. Farnesyltransferase and geranylgeranyltransferase I are among the very few enzymes that have a coordination sphere of this type.[3,14,24]

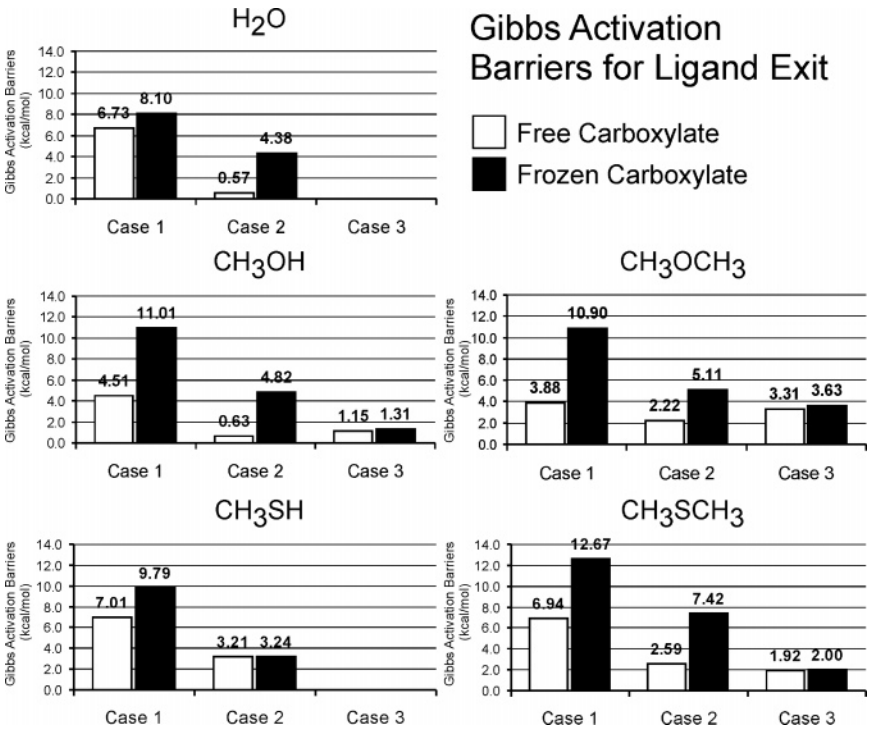

Figure 5. Relation of the Gibbs activation barriers for ligand exit with a free and a frozen carboxylate group (Gibbs energies approximately calculated in this latter case) for the several coordination spheres and ligands studied.

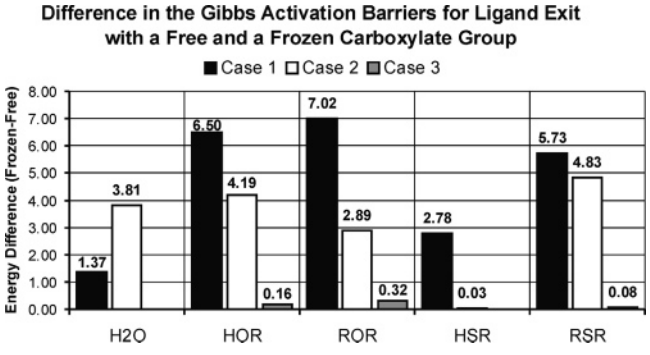

Figure 6. Difference in the Gibbs activation barriers (kcal/mol) for ligand exit with a free and a frozen carboxylate group (Gibbs energies approximately calculated in this latter case) for the several coordination spheres and ligands studied. R corresponds to a CH_3 group.

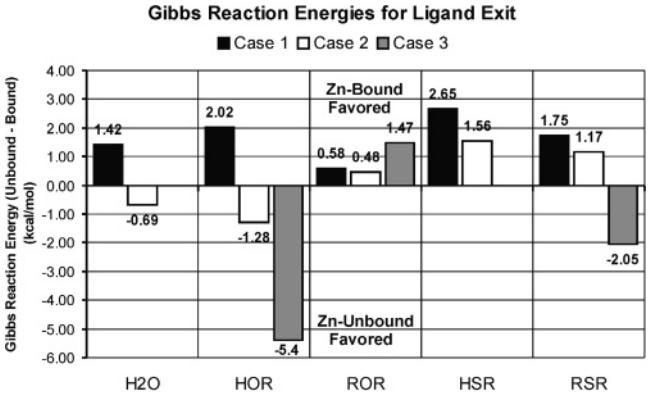

Figure 7. Relation of the Gibbs reaction energies for ligand exit for the several coordination spheres and ligands studied. R corresponds to a CH_3 group.

For the case 3 sphere, which contains one carboxylate and two cysteine residues (overall charge −1), ligand coordination is not energetically favored. In fact, for the set of ligands studied, the ligand displacement process from the Zn center has been shown to be exothermic and to proceed through a remarkably small activation barrier. For two of the ligands, no Zn-bound minimum was obtained at all. Hence, no carboxylate shift is required to promote a fast ligand exit, as ligand coordination to Zn is extremely feeble (Figure 3). These aspects render case 3 a bad coordination environment for a catalytic Zn sphere, at least for mechanisms involving molecules of the type of the five ligands studied. Coherent with this fact, no catalytic Zn center with such combination of ligands has been reported in the literature.[2,3,14,23,24]

Conclusions

Even though in the real biological systems the relative stability of monodentate and bidentate minima and the Gibbs activation barriers for ligand exit will be influenced by the specific enzymatic environment surrounding each metal center, some very important conclusions about the intrinsic characteristics of each metal center can be drawn from the set of results obtained.

The carboxylate-shift mechanism is an important phenomenon in Zn systems that allows for a fast and extremely controlled process of ligand exchange through a subtle alteration in the metal coordination form of a carboxylate ligand that lowers the Gibbs activation barrier for the process. The magnitude of such an effect depends on the exact combination of amino acid residues at the Zn coordination sphere and to a lesser extent on the identity of the very own ligand to be exchanged. A particular combination of residues containing a histidine and a cysteine and a generic carboxylate ligand (Asp or Glu) enables the fastest ligand exchange processes, with both bound and unbound minima at a notably close energetic proximity, and the lowest activation barriers. In a Zn coordination sphere containing two histidines and the carboxylate ligand (the most common

combination of ligands in catalytic Zn enzymes, particularly when L = H_2O), ligand exchange has significantly higher activation barriers, even with a carboxylate-shift mechanism, and ligand displacement is typically an endothermic process. Finally, the Zn coordination sphere that contains two cysteine residues in addition to the carboxylate ligand does not suffer carboxylate shift at all, and ligand coordination is not energetically favored.

These conclusions seem to suggest that Zn enzymes having a Zn coordination sphere containing a cysteine, a histidine, and a carboxylate ligand (such as farnesyltransferase and geranylgeranyltransferase I, for example) have a unique combination of ligands that provides additional versatility and easier ligand exchange to the already flexible coordination environment characteristic of Zn enzymes in general.

Acknowledgment. We thank the Fundação para a Ciência e a Tecnologia (FCT) for financial support (POCI/QUI/61563/2004). S.F.S. also acknowledges the FCT for a doctoral scholarship (SFRH/BD/12848/2003).

Supporting Information Available: Complete refs 15 and 52. Comparison of the performance of the B3LYP functional in the treatment of Zn complexes for geometry optimizations and for energy calculations against the B1B95, B97-2, BP86, and BPW91 functionals. Variation of the Zn−O1 and Zn−O2 distances with ligand exit for the several coordination spheres (cases 1, 2, and 3) and ligands L. Relative Gibbs energies for all the stationary states determined from both free and frozen scans for all five ligands and three coordination environments studied. Cartesian coordinates of all the initial minima. This material is available free of charge via the Internet at http://pubs.acs.org.

JA067103N